

Article

Laser Texturing of Tungsten Carbide (WC-Co): Effects on Adhesion and Stress Relief in CVD Diamond Films

Argemiro Pentian Junior ^{*}, José Vieira da Silva Neto , Javier Sierra Gómez , Evaldo José Corat 
and Vladimir Jesus Trava-Airoldi

National Institute for Space Research—INPE, São José dos Campos 12227-010, Brazil;
jvneto.ifsp@gmail.com (J.V.d.S.N.); javiersierra25@gmail.com (J.S.G.); evaldo.corat@inpe.br (E.J.C.);
vladimir.airoldi@inpe.br (V.J.T.-A.)

^{*} Correspondence: argemiro.junior@inpe.br

Abstract

This study proposes a laser texturing method to optimize adhesion and minimize residual stresses in CVD diamond films deposited on tungsten carbide (WC-Co). WC-5.8 wt% Co substrates were textured with quadrangular pyramidal patterns (35 μm) using a 1064 nm nanosecond-pulsed laser, followed by chemical treatment (Murakami's solution + *aqua regia*) to remove surface cobalt. Diamond films were grown via HFCVD and characterized by Raman spectroscopy, EDS, and Rockwell indentation. The results demonstrate that pyramidal texturing increased the surface area by a factor of 58, promoting effective mechanical interlocking and reducing compressive stresses to -1.4 GPa. Indentation tests revealed suppression of interfacial cracks, with propagation paths deflected toward textured regions. The pyramidal geometry exhibited superior cutting post-deposition cooling time for stress relief from 3 to 1 h. These findings highlight the potential of laser texturing for high-performance machining tool applications.

Keywords: laser surface texturing; CVD diamond films; adhesion enhancement; residual stress relief; mechanical interlocking



Academic Editor: Aleksey Yerokhin

Received: 31 March 2025

Revised: 8 May 2025

Accepted: 17 May 2025

Published: 30 July 2025

Citation: Junior, A.P.; Silva Neto, J.V.d.; Gómez, J.S.; Corat, E.J.; Trava-Airoldi, V.J. Laser Texturing of Tungsten Carbide (WC-Co): Effects on Adhesion and Stress Relief in CVD Diamond Films. *Surfaces* **2025**, *8*, 54. <https://doi.org/10.3390/surfaces8030054>

Copyright: © 2025 by the authors. Licensee MDPI, Basel, Switzerland. This article is an open access article distributed under the terms and conditions of the Creative Commons Attribution (CC BY) license (<https://creativecommons.org/licenses/by/4.0/>).

1. Introduction

Since the discovery of chemical vapor deposition of diamond on non-diamond substrates in 1982 by Matsumoto et al. [1], diamond coatings have attracted global interest due to exceptional properties such as hardness and thermal conductivity [2]. However, the adhesion of these films to tungsten carbide (WC-Co) faces critical challenges: (i) thermal incompatibility between diamond and substrate, generating high residual stresses [3], and (ii) cobalt migration to the interface, which inhibits diamond nucleation [4]. Traditional methods like sandblasting or chemical treatment remove Co but often fail to control surface roughness or relieve stresses efficiently.

In this context, laser texturing emerges as a promising alternative, enabling the creation of customized micro/nanostructures that enhance mechanical anchoring through an interlocking effect and improve thermal stress dissipation. These precisely engineered structures (ranging from micro to nanoscale) promote superior adhesion by creating a mechanical self-locking effect at the interface [5]. Furthermore, the strategic design of these textured patterns compensates for the thermal mismatch between diamond (CTE: $1.0\text{--}1.5 \times 10^{-6} \text{ K}^{-1}$) and WC-Co (CTE: $4.5\text{--}6.0 \times 10^{-6} \text{ K}^{-1}$), converting post-deposition cooling stresses into beneficial compressive forces that reinforce coating adhesion. The study evaluates the

impact of laser pyramidal texturing on WC-Co regarding surface area/volume increase, CVD diamond adhesion, and residual stress reduction. It explores the relationship between surface roughness and performance under simulated operational conditions.

The results of this study contribute to the development of CVD diamond coatings with superior performance for industrial applications requiring enhanced adhesion and prolonged durability. The laser texturing approach demonstrates potential for optimizing high-performance cutting tools and mechanical components subjected to severe operating conditions, where coating–substrate interface integrity is crucial for system lifespan.

2. Materials and Methods

For this study, we used WC-5.8 wt% Co TNMA 160408 inserts from the manufacturer BRASSINTER (São Paulo, Brazil), with a grain size of 0.5 μm and geometry as shown in Figure 1, along with dimensions provided in Table 1. The substrates were textured with a quadrangular pyramidal geometric pattern using a 1064 nm wavelength laser featuring a maximum pulse energy of 1 mJ, repetition rate of 2–200 kHz, pulse duration of 100 ns, and power ranging from 20 to 100 W. Following laser texturing, the samples underwent chemical treatment to selectively remove cobalt. This step involved Murakami’s solution ($\text{K}_3[\text{Fe}(\text{CN})_6] + \text{KOH} + \text{H}_2\text{O}$) and “aqua regia” solution ($\text{HNO}_3/\text{HCl} = 1:3$), following the methodology described elsewhere [6].

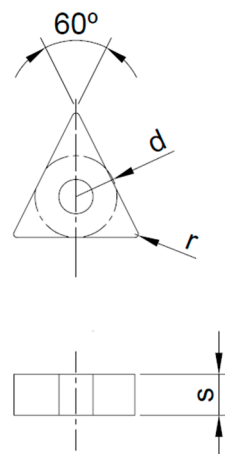


Figure 1. Geometry of the inserts used in the development of the work. Adapted from Ref. [7]. Copyright 2023, Brassinter.

Table 1. Measurements of the inserts used in the development of the work. Adapted from Ref. [7]. Copyright 2023, Brassinter.

ISO	d (mm)	r (mm)	s (mm)
TNMA 160408	9.525	4.76	0.8

After texturing, the inserts were evaluated by scanning electron microscopy (SEM) and energy dispersive X-ray spectroscopy (EDS) to analyze the cobalt level on the surface and its morphology.

To increase the nucleation rate, the inserts were subjected to a seeding procedure with 30 min immersion in a solution containing 4 nm diamond powder dispersed in deionized water along with an anionic polymer (PSS—sodium polystyrenesulfonate) and another 30 min in a cationic polymer PDDA, also containing diamond nanoparticles. After this period, the excess solution was removed using deionized water [8]. Both PSS and

PDDA polymers were acquired from the commercial supplier Sigma Aldrich Co (St. Louis, MO, USA).

For diamond film growth, a Hot Filament Chemical Vapor Deposition (HFCVD) reactor shown in Figure 2a was used. The reactor setup consisted of five tungsten filaments with 0.85 mm diameter, uniformly spaced at 4.5 mm intervals from each other as shown in Figure 2b, and positioned 3.2 mm from the insert. These filaments were maintained at an average power of 450 W with the insert temperature at 850 °C, measured by a type J thermocouple, during all time of deposition.

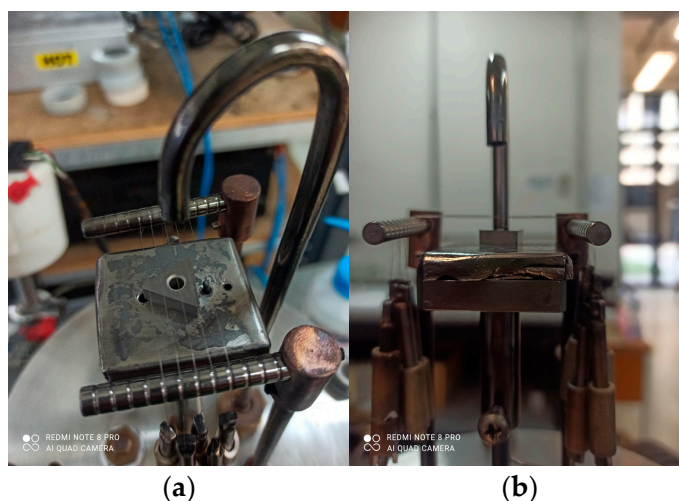


Figure 2. Configuration of the hot-filament chemical vapor deposition (HFCVD) reactor: (a) top view showing filament arrangement and (b) front view detailing the 3.2 mm filament-insert gap.

It is worth noting that the process gases interact with the filament, resulting in carbon absorption and the formation of tungsten carbide [9–11]. This leads to an increase in filament resistivity and subsequently higher temperatures due to the increased available power, resulting in constant adjustment of the supplied current up to when the nucleation is completed. The gas concentration remained fixed at a ratio of 98% hydrogen (H₂) and 2% methane (CH₄). The gases were stored separately and combined after passing through controllable flow meters before being introduced into the water-cooled reactor's vacuum chamber. The pressure inside of the chamber was kept at 50 Torr during all the experiment. The filament assembly was powered by an adjustable DC power supply.

Following diamond coating deposition, the inserts were morphologically characterized by scanning electron microscopy (SEM), revealing microstructural parameters such as grain size, surface morphology, and coating uniformity. The BET (gas desorption) technique was employed for surface area quantification, being particularly effective for complex structures due to its molecular adsorption principle. Raman spectroscopy identified the characteristic film peak (~1332 cm⁻¹), enabling residual stress calculation through the Ager and Drory equation.

The study focused on the cutting edge region due to its functional relevance, particularly regarding film adhesion and stress distribution. Three-dimensional volume analysis was performed using Alicona's Mex software Version 6 combined with SEM images, complementing the surface characterization. Additionally, Rockwell indentation tests evaluated film–substrate adhesion by analyzing indentation effects. The integration of these techniques established relationships between deposition parameters and the coating's morphological/mechanical properties.

3. Results and Discussions

3.1. Morphology and Characterization of WC-Co Substrates After Texturing

The examination of the textured surface area allows us to assess the extent of modification and the distribution of irregularities resulting from the texturing process. Furthermore, evaluating the volume of asperities formed provides insights into the depth and scope of the topographical changes. These measurements have significant implications for a variety of applications, including coating adhesion and tribological performance, as surface roughness directly influences friction, wear resistance, and mechanical interlocking of deposited layers.

Figure 3 shows burrs along the channel edges and a layer of resolidified material deposited over the textured surface. Despite these superficial irregularities, the underlying pattern geometry remains intact and conforms to the intended design. The excess material and burrs will be eliminated in a subsequent chemical treatment step, fully restoring the original texture.

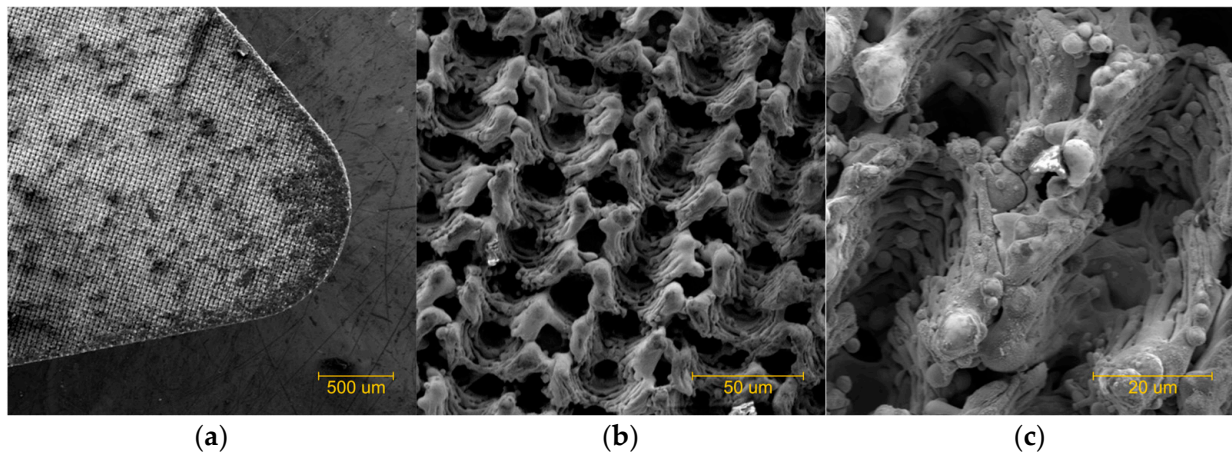


Figure 3. (a) Square profile of 35 μm after texturing, (b) detail of the relief, (c) detail of the channel and textured top.

When laser fluences, that is, energy densities, are applied above the ablation threshold, heat transfer beyond the area irradiated by the laser pulse ends up creating this effect [12,13]. Part of the molten material solidifies again, forming geometric imperfections and burrs. As a result of the interaction between the laser and the insert surface, the generated heat causes cobalt to migrate to the surface, increasing its density. EDS analysis indicated an increase from 5.8% to 9.3%, representing a 60.34% increase in surface cobalt concentration.

Excessively long or intense texturing processes can lead to the formation of undesirable phases, such as oxides or intermediate carbides, compromising the quality of the deposited diamond film, as reported in the literature [13,14]. Therefore, XRD analysis of the samples (Figure 4) was performed and compared with the reference standard composed of tungsten carbide (Figure 5), revealing small additional peaks of cobalt tungsten carbide ($\text{Co}_3\text{W}_3\text{C}$). This indicates that the material's chemical composition and atomic organization remained stable.

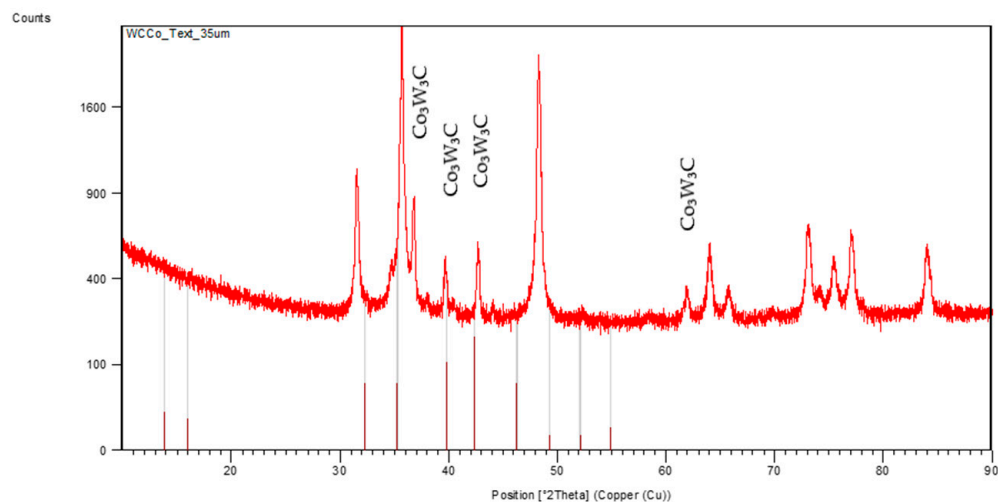


Figure 4. XRD of the surface of the 35 μm textured insert.

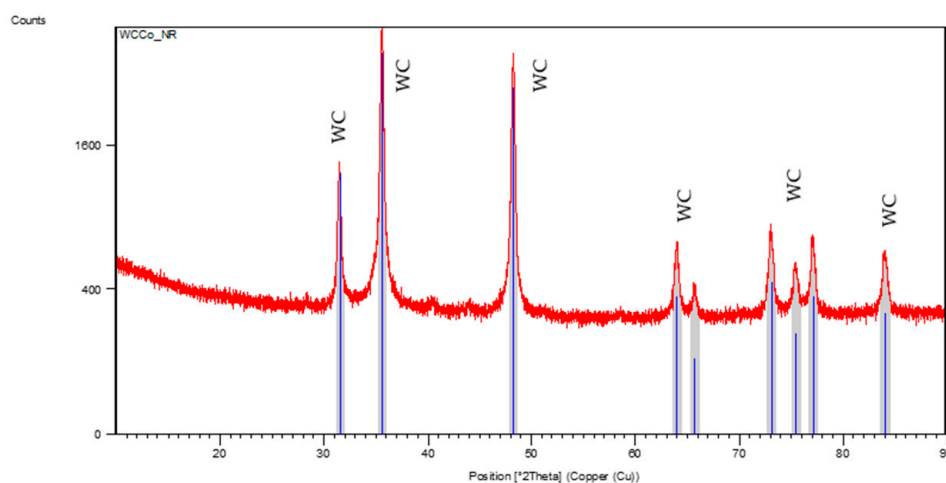


Figure 5. XRD of the surface of the pre-textured insert.

3.2. Morphology and Characterization of WC-Co Substrates After Cobalt Removal

For the preparation prior to diamond film growth, the WC-Co inserts underwent a two-stage chemical treatment for cobalt removal, as described by Fraga et al. [6]. The treatment sequence consisted first of immersion in Murakami's solution ($\text{K}_3[\text{Fe}(\text{CN})_6] + \text{KOH} + \text{H}_2\text{O}$), followed by treatment with aqua regia (HNO_3/HCl at 1:3 ratio), resulting in a final surface roughness of $5.20 \mu\text{m}$. Figure 6 shows the results obtained after this surface preparation process.

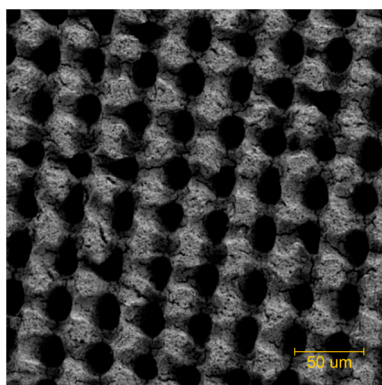


Figure 6. Morphological changes after chemical treatment.

The analysis of surface area and volume contributes to understanding the topographical changes caused by texturing. The resulting three-dimensional geometry, with pits and recesses, requires specific characterization methods. The BET (gas desorption) technique was chosen for its ability to quantify surface area in complex structures, based on the principle of molecular adsorption. Unlike conventional methods, this approach properly characterizes the complex morphology of textured surfaces. Based on the obtained results, relationships can be established between topographical parameters and functional performance.

In Table 2, we can observe the area gain evolution by comparing the as-received area with the textured area after the preparation step for diamond film deposition.

Table 2. Area measurements.

Texturing (μm)	As-Received Area (m^2/g)	Post-Treatment Area (m^2/g)
35	0.004	0.232

The laser texturing process promoted a significant increase in the surface area of the WC-Co inserts, as quantified by the BET technique using a Quantachrome Instruments Model 27-E analyzer. The results demonstrated that the pyramidal pattern generated a 58-fold increase in surface area compared to the non-textured substrate (from $0.004 \text{ m}^2/\text{g}$ to $0.232 \text{ m}^2/\text{g}$). This gain is directly associated with the formation of complex micro and nanostructures (peaks, channels, and recesses), which expand the effective surface for diamond film nucleation and mechanical anchoring. Such increase is particularly relevant for applications where interfacial adhesion is critical, such as in high-performance machining tools.

The three-dimensional analysis, performed using Alicona's Mex 6.0 Software combined with scanning electron microscopy (SEM) images, revealed that the chemical treatment for cobalt removal caused significant changes in the already textured surface volume, as shown in Table 3. The data indicated a reduction from $4,846,670.04 \mu\text{m}^3$ to $2,340,265.09 \mu\text{m}^3$, while preserving the controlled cavities (pits and recesses) previously created by the texturing process. Although this modification represents a volumetric decrease, it proved to be structurally advantageous: the additional recesses contributed to more uniform stress distribution.

Table 3. Volume area measurements.

Texturing (μm)	Pre-Treatment Area (μm^3)	Post-Treatment Area (μm^3)
35	4,846,670.04	2,340,265.09

A new analysis of the surface after removal of the re-solidified material and chemical treatment indicated that anchoring structures were created in synergy with micropits and recesses. In addition to altering the surface topography, the texturing and chemical treatment also prepare a suitable topography for the deposition of polycrystalline diamond films. The micropits improve film adhesion and functionality by creating anchoring regions that assist in the chemical bonding and mechanical trapping of the diamond film to the insert surface. During deposition, the controlled profile irregularities provide an expanded surface area for film fixation and also function as stress dissipators that absorb part of the energy, thereby increasing coating stability and minimizing the probability of delamination due to mechanical and/or thermal stresses. The presence of micropits also assists in the uniform distribution of deposited material when the film deposition rate is adjusted, leading to a reduction in film thickness irregularities. One can speculate that these cavities work as guides, increasing the diamond particle nucleation density and stimulating more

uniform growth of subsequent layers. These cavities also function as templates that control diamond particle nucleation, promote uniform layer growth, and optimize interfacial stress distribution.

3.3. Morphology and Characterization of Diamond Films

The scanning electron microscopy (SEM) analysis, conducted using a JEOL JSM-5310 microscope, as shown in Figure 7, revealed that the diamond film, deposited over 25 h via HFCVD at a growth rate of 1.08 $\mu\text{m}/\text{h}$, showed a homogeneous columnar structure over the textured surface, completely filling the pyramidal structures and their recesses. As evidenced in Figure 7, the complete filling of the textured pattern demonstrates the deposition process's ability to promote controlled material growth even over complex topography. The SEM images further show the film's polycrystalline structure, with uniformly distributed grains of 12 to 14 μm , along with a cohesive and continuous film–substrate interface showing no apparent discontinuities.

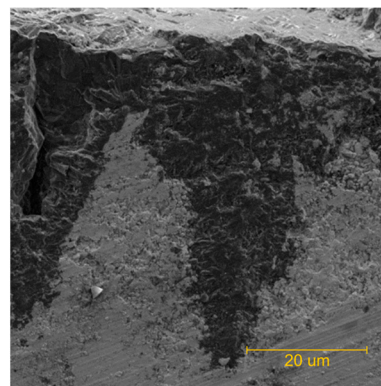


Figure 7. Cross-section of the insert's cutting edge after deposition.

3.4. Mechanical Interlocking at the Interface

The microstructural analysis revealed an effective mechanical interlocking mechanism between the diamond film and the textured substrate as shown in Figure 8. The inclined faces, with different roughness of the pyramids and inner surfaces itself create a three-dimensional anchoring structure capable of distributing mechanical stresses throughout the interface. This geometric arrangement dissipates shear and tensile forces, preventing local stress concentrations that could compromise the system's integrity.

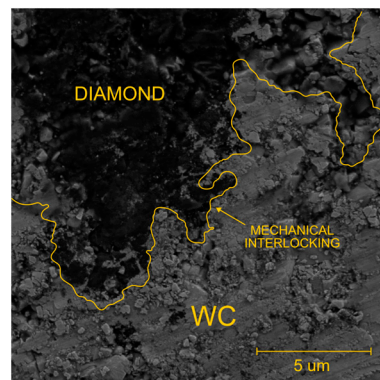


Figure 8. Cross-section of the diamond film with detail of the mechanical interlocking at the interface of diamond with WC-Co.

The interlocking proved particularly effective in maintaining interfacial stability, even under high loads or significant thermal variations. The three-dimensional configuration

promotes multidirectional stress accommodation, explaining the delamination resistance observed in indentation tests. This mechanism is fundamental for applications requiring durability under extreme operational conditions, such as in high-performance cutting tools where interface integrity is critical. The system's efficiency is enhanced by the combination of diamond's intrinsic properties and the substrate's controlled topography.

3.5. Analysis of the Roughness of the Diamond Film

The surface roughness characterization ($R_a = 11.55 \mu\text{m}$), as shown in Figure 9 of the diamond film, reveals a compromise between adhesion and functional performance. While the underlying pyramidal texturing favors mechanical anchoring of the coating, the long deposition time results in roughness values higher than ideal for fine finishing operations (for example, $0.4\text{--}1.6 \mu\text{m}$, $0.4\text{--}1.6 \mu\text{m}$). This characteristic limits the film's application to contexts where surface finish requirements prevail over wear resistance.

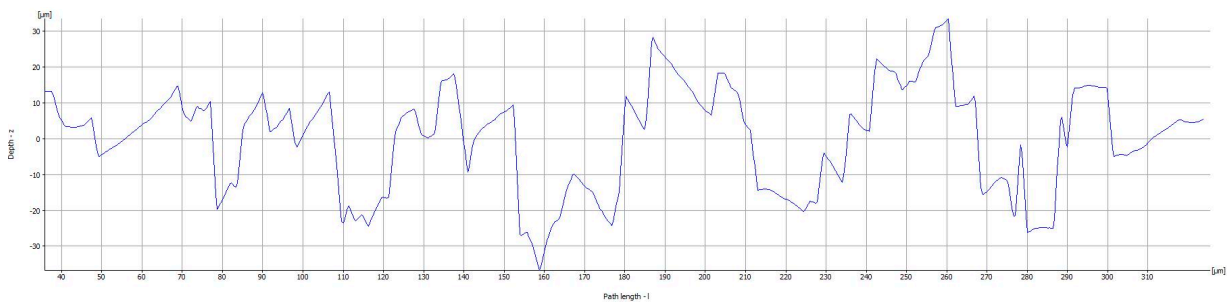


Figure 9. Profile of the roughness of the diamond film.

However, for conventional cutting tools where roughness transfer to the workpiece is less critical, the film maintains adequate functional performance. This analysis highlights the importance of topographic control in diamond coating development, suggesting that future process optimizations should seek to balance the benefits of texturing with surface finish requirements for specific applications.

3.6. Analysis of Residual Stress

Raman spectroscopy analysis, performed using a LabRAM HR Evolution system, confirmed the high crystalline quality of the diamond film, evidenced by the characteristic peak at 1334.45 cm^{-1} , as shown in Figure 10, corresponding to the sp^3 carbon hybridization in the diamond structure. The narrow and intense peak indicates high material purity and crystallinity, with its width reflecting the uniform size of crystalline grains. Application of the Ager and Drory equation [15] revealed compressive residual stresses of -1.389 GPa , demonstrating the effectiveness of pyramidal texturing in promoting homogeneous growth, as evidenced by the low stress value dispersion and, also, by the absence of peaks associated with amorphous or graphitic structure.

The pyramidal geometry provides significant advantages by eliminating right angles, as its inclined faces distribute stresses uniformly. This configuration removes critical points, enhances mechanical resistance, and increases the effective surface area, substantially improving film–substrate adhesion. As a result, even under compressive stresses, the system maintains superior performance, combining durability and structural stability.

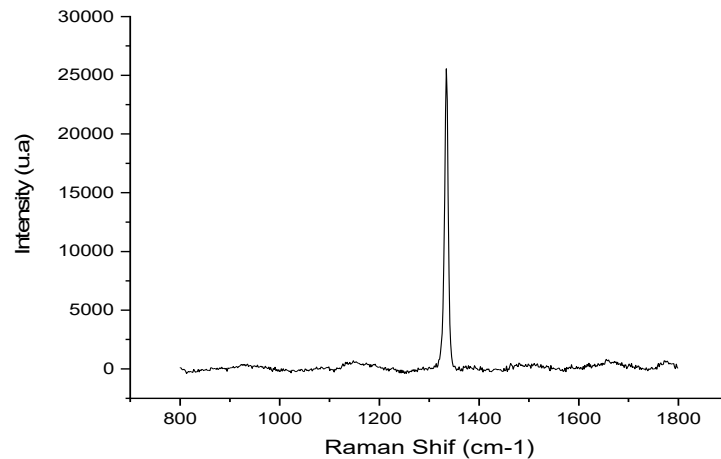


Figure 10. Raman spectrum of diamond on the cutting edge region of the insert.

3.7. Indentation Tests

The Rockwell indentation tests were performed using a Reicherter hardness tester, model BVR. A normal load of 150 kg was applied with a dwell time of 10 s, using a diamond Rockwell conical indenter with a tip radius of 0.2 mm and an opening angle of 120° .

The indentation tests confirmed the excellent adhesion of the diamond film deposited on the pyramidal texturing. The observed sink-in phenomenon (Figure 11)—the indentation of the rigid film (modulus ~ 1050 GPa) into the WC substrate (~ 600 GPa)—occurred in a controlled manner, demonstrating good interfacial adhesion and structural integrity. The absence of significant delamination or radial cracks at the impression edges attests to the effectiveness of the texturing in resisting concentrated loads, reinforcing the quality of the obtained film.

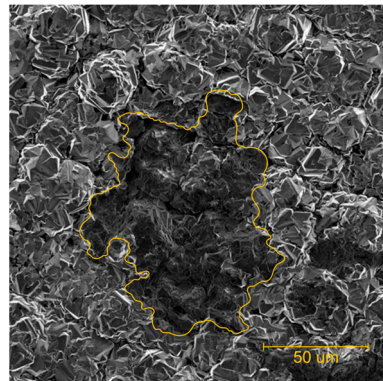


Figure 11. Microstructural characterization of the indentation profile on the diamond-coated textured surface: deformation behavior and interfacial adhesion.

The pyramidal geometry proved fundamental for superior mechanical performance, effectively dissipating stresses through its inclined faces while maintaining interface stability even under deformation. This combination of diamond's intrinsic properties and topographic optimization results in a coated system with adequate resistance for applications under extreme loads.

3.8. Optimization of the Cooling Process Through Pyramidal Texturing

The conventional thermal stress relief process, which involves gradual removal of the carbon precursor and controlled three-hour cooling, was significantly optimized through the adoption of pyramidal texturing. This new geometry reduces cooling time to just one hour or less while preserving system integrity, due to three main mechanisms. First, efficient

thermal dissipation is promoted by the inclined pyramid faces, which ensure uniform heat distribution and increase surface area by 58 times compared to non-textured substrates, accelerating heat transfer and eliminating local gradients that could generate residual stresses. Second, the three-dimensional pyramid structure provides multiple physical interconnection points between film and substrate, preventing failures during thermal cycles; the mechanical interlocking demonstrated in indentation tests proves effective against thermally induced delamination. Finally, the absence of orthogonal corners enables multidirectional thermal accommodation, avoiding the stress concentrators common in cubic texturing patterns, as evidenced by experimental data showing average residual stresses of -1.4 GPa at the cutting edge. This optimization did not compromise film quality, as verified by Raman spectroscopy showing a peak at 1334.45 cm^{-1} , and by mechanical tests that maintained all advantages of conventional deposition while increasing thermal cycle efficiency by 66%. This solution is particularly valuable for industrial-scale cutting tool production, where time and consistency are critical factors.

4. Conclusions

This study demonstrated that laser texturing of tungsten carbide (WC-Co) with quadrangular pyramidal patterns is an effective approach to enhance adhesion and reduce residual stresses in CVD diamond films. The texturing process increased surface area by 58 times, promoting efficient mechanical interlocking between the film and substrate, which resulted in significantly improved adhesion. Furthermore, the pyramidal geometry proved advantageous for thermal stress dissipation, reducing compressive stresses to -1.4 GPa and decreasing post-deposition cooling time from 3 to 1 h.

Rockwell indentation tests confirmed the interface robustness, showing no delamination or radial cracks, demonstrating the texturing's effectiveness in resisting concentrated loads. Raman spectroscopy analysis also revealed the high crystalline quality of the diamond film, with a characteristic peak at 1334.45 cm^{-1} , confirming the purity and crystallinity of the deposited material.

Therefore, laser texturing of WC-Co has proven to be a promising technique for industrial applications requiring diamond coatings with high adhesion and durability, such as machining tools. The study's results pave the way for further process optimizations to balance roughness and functional performance for specific applications. The proposed approach not only improves coating quality but also enhances process efficiency, making it viable for industrial-scale production.

Author Contributions: Conceptualization, A.P.J.; methodology, A.P.J.; software, A.P.J.; validation, V.J.T.-A.; formal analysis, A.P.J.; investigation, A.P.J.; resources, E.J.C.; data curation, A.P.J.; writing—original draft, A.P.J.; review V.J.T.-A. and J.V.d.S.N. and J.S.G.; visualization, J.V.d.S.N. and J.S.G.; supervision, V.J.T.-A.; project administration, E.J.C.; funding acquisition, E.J.C., contributed equally to this work. All authors have read and agreed to the published version of the manuscript.

Funding: This research was supported by FAPESP [2019/18572-7].

Institutional Review Board Statement: Not applicable.

Informed Consent Statement: Not applicable.

Data Availability Statement: The original contributions presented in the study are included in the article, further inquiries can be directed to the corresponding author.

Conflicts of Interest: The authors declare no conflicts of interest.

References

1. Matsumoto, S.; Sato, Y.; Kamo, M.; Setaka, N. Vapor Deposition of Diamond Particles from Methane. *Jpn. J. Appl. Phys.* **1982**, *21*, L183–L185. [CrossRef]
2. Zhang, C.; Vispute, R.D.; Fu, K.; Ni, C. A review of thermal properties of CVD diamond films. *J. Mater. Sci.* **2023**, *58*, 3485–3507. [CrossRef]
3. Gunnars, J.; Alahelisten, A. Thermal stresses in diamond coatings and their influence on coating wear and failure. *Surf. Coat. Technol.* **1996**, *80*, 303–312. [CrossRef]
4. Lu, Y.; Deng, J.; Wang, R.; Wu, J.; Meng, Y. Tribological performance of micro textured surface machined by Nd:YAG laser with different incident angle. *Opt. Laser Technol.* **2022**, *148*, 107768. [CrossRef]
5. Fatima, A.; Whitehead, D.J.; Mativenga, P.T. Femtosecond laser surface structuring of carbide tooling for modifying contact phenomena. *Proc. Inst. Mech. Eng. Part B J. Eng. Manuf.* **2014**, *228*, 1325–1337. [CrossRef]
6. Fraga, M.A.; Contin, A.; Rodríguez, L.A.; Vieira, J.; Campos, R.A.; Corat, E.J.; Airoidi, V.T. Nano- and microcrystalline diamond deposition on pretreated WC-Co substrates: Structural properties and adhesion. *Mater. Res. Express* **2016**, *3*, 025601. [CrossRef]
7. São Paulo, S.P. Product Catalog/Technical Information. Available online: http://www.brassinter.com.br/downloads/pastilhas_torneamento.pdf (accessed on 8 May 2025).
8. Campos, R.A.; Contin, A.; Trava-Airoidi, V.J.; Moro, J.R.; Barquete, D.M.; Corat, E.J. CVD diamond films growth on silicon nitride inserts (Si₃N₄) with high nucleation density by functionalization seeding. *Mater. Sci. Forum* **2012**, *727–728*, 1433–1438. [CrossRef]
9. Haubner, R.; Lux, B. Diamond growth by hot-filament chemical vapor deposition: State of the art. *Diam. Relat. Mater.* **1993**, *2*, 1277–1294. [CrossRef]
10. Moustakas, T.D. The role of the tungsten filament in the growth of polycrystalline diamond films by filament-assisted CVD of hydrocarbons. *Solid State Ion.* **1989**, *32–33*, 861–868. [CrossRef]
11. Okoli, S.; Haubner, R.; Lux, B. Carburization of tungsten and tantalum filaments during low-pressure diamond deposition. *Surf. Coat. Technol.* **1991**, *47*, 585–599. [CrossRef]
12. Vázquez, J.M.; Salguero, J.; Del Sol, I. Texturing design of WC-Co through laser parameter selection to improve lubricant retention ability of cutting tools. *Int. J. Refract. Met. Hard Mater.* **2022**, *107*, 105880. [CrossRef]
13. Zhang, Z.; Lu, W.Z.; He, Y.F.; Zhou, G.H. Research on optimal laser texture parameters about antifriction characteristics of cemented carbide surface. *Int. J. Refract. Met. Hard Mater.* **2019**, *82*, 287–296. [CrossRef]
14. Barletta, M.; Rubino, G.; Valle, R.; Polini, R. Chemical vapor deposition of highly adherent diamond coatings onto co-cemented tungsten carbides irradiated by high power diode laser. *ACS Appl. Mater. Interfaces* **2012**, *4*, 694–701. [CrossRef]
15. Ager, J.W.; Drory, M.D. Quantitative measurement of residual biaxial stress by Raman spectroscopy in diamond grown on a Ti alloy by chemical vapor deposition. *Phys. Rev. B* **1993**, *48*, 2601–2607. [CrossRef]

Disclaimer/Publisher’s Note: The statements, opinions and data contained in all publications are solely those of the individual author(s) and contributor(s) and not of MDPI and/or the editor(s). MDPI and/or the editor(s) disclaim responsibility for any injury to people or property resulting from any ideas, methods, instructions or products referred to in the content.